

Explainable Spatial-Temporal Modeling and Ensemble Modeling for Predicting Food Security

RONALD ATUHAIRE¹, (Member, IEEE), EDWARD KABOGGOZA², AND GEORGE SSEMAGANDA.³, (Member, IEEE)

¹Makerere University, College of Computing and Information Sciences, Kampala, Uganda (e-mail: atuhaire.ronald@students.mak.ac.ug)

²Makerere University, College of Computing and Information Sciences, Kampala, Uganda (e-mail: kaboggoza.edward@students.mak.ac.ug)

³Makerere University, College of Computing and Information Sciences, Kampala, Uganda (e-mail: george.ssemaganda@students.mak.ac.ug)

Corresponding author: Ronald Atuhaire (e-mail: atuhaire.ronald@students.mak.ac.ug).

ABSTRACT Accurate prediction of food security is critical for mitigating climate-induced agricultural risks, yet existing methods struggle to reconcile spatiotemporal complexity with interpretability. This study addresses this gap through a comprehensive evaluation of machine learning paradigms—baseline models, ensemble techniques, and spatial-temporal graph neural networks—for rainfall-driven food security forecasting in Uganda. We propose a unified framework integrating 15 distinct models, ranging from linear regressors (Ridge, Lasso) and tree-based ensembles (XGBoost, Gradient Boost) to a novel Spatial Graph Attention Network (GAT) enhanced with multi-head temporal attention. We also implemented Temporal-GNN which integrates graph convolutional networks (GCN) with gated recurrent units (GRU) to model spatiotemporal patterns in rainfall-food security relationships. To bridge the transparency gap in AI-driven predictions, SHAP (SHapley Additive exPlanations) and LIME (Local Interpretable Model-agnostic Explanations) are systematically applied across all models, quantifying the influence of climatic drivers such as immediate rainfall intensity ($r1h$), seasonal fluctuations, and pressure gradients (rfq).

Key advancements include: XGBoost achieving state-of-the-art performance ($R^2 = 0.9949$, $MAE = 1.4067$), surpassing baseline models by 14.3% in predictive accuracy; The Spatial GAT model demonstrating robust temporal dependency capture ($MSE = 0.2092$, $MAE = 0.337$), offering granular spatiotemporal insights despite a lower R^2 (0.7801); and Model-agnostic explainability revealing divergent feature importance—linear models prioritize temperature, whereas ensembles emphasize atmospheric pressure dynamics. A reproducible pipeline incorporating spatial cross-validation, CUDA-accelerated training, and interactive XAI visualization is introduced to enhance methodological rigor.

Policymakers benefit from actionable trade-offs: The Voting Regressor ($MAE = 2.2880$) balances interpretability and performance, while the Spatial GAT enables localized, climate-resilient planning. This work advances scalable food security analytics by unifying statistical robustness with temporal dependency modeling, setting the stage for hybrid ensemble-GAT architectures in future research.

INDEX TERMS Climate Change, Ensemble Learning, Explainable AI, Food Security, Spatial-Temporal Modeling, Time-Series Forecasting

I. INTRODUCTION

FOOD security is one of the most critical challenges facing the world today, with far-reaching consequences for health, livelihoods, and economic development. Uganda's economy heavily depends on agriculture, which employs over 70% of the population and contributes about 24% to the national Gross Domestic Product (GDP) [30]. Both rural

and urban communities rely on agriculture as a key source of sustenance and income. However, the country's dependence on rain-fed farming exposes its food systems to significant risks. Variations in climate, such as erratic rainfall, extended droughts, and frequent floods, pose direct threats to crop yields and food supply chains. These disruptions disproportionately impact regions dominated by smallholder farmers,

exacerbating food insecurity and straining rural livelihoods.

The growing unpredictability of weather patterns, fueled by climate change, has made forecasting food security increasingly complex. Shifting rainfall seasons, rising temperatures, and extreme climatic events disrupt agricultural cycles, destabilizing both production and markets. Understanding how environmental, spatial, and temporal factors interact is critical to identifying vulnerable areas and implementing targeted interventions. However, this complexity poses significant challenges to effective prediction.

Traditional predictive approaches, including models like Linear Regression, Random Forest, Decision Trees, and Gradient Boosting, have provided valuable insights into agricultural and climatic trends. Yet, these methods often fall short when dealing with the interconnected spatial and temporal elements critical to long-term forecasting. Their reliance on static datasets limits their ability to capture dynamic changes, such as regional climate shifts or seasonal variability. Additionally, the "black box" nature of many machine learning models makes it difficult to interpret their outputs, reducing their usefulness for policymakers who require transparent and actionable data.

Recognizing these gaps, researchers have increasingly turned to spatial-temporal modeling as a more comprehensive approach. Unlike traditional methods, spatial-temporal models analyze patterns across both time and geography, enabling a deeper understanding of how climatic changes affect food production. For instance, these models can map rainfall trends across districts over multiple years, helping to identify areas at higher risk of food insecurity. By capturing correlations and causal relationships, spatial-temporal modeling provides a foundation for proactive, data-driven agricultural strategies that are better equipped to address Uganda's food security challenges.

The integration of time-series data into spatial-temporal models offers additional benefits by capturing the dynamic evolution of climatic and agricultural variables. Time-series data, which captures observations sequentially over time, is invaluable for identifying trends, cycles, and seasonal patterns. In the context of food security, analyzing time-series data enables predictions of key variables like rainfall, temperature, and crop yields, allowing for early warnings and timely interventions. However, effectively utilizing time-series data requires advanced modeling techniques that can handle the complexities of high-dimensional datasets and nonlinear relationships, which are often present in agricultural and climatic data.

In our earlier work on Transparent Multimodeling for Climatic Geo-Intelligence in Predicting Food Insecurity [4], we identified rainfall patterns as a critical factor influencing food insecurity in Uganda. Rainfall plays a pivotal role in various stages of agriculture, from seed germination and

crop growth to harvesting and storage. Regions experiencing erratic rainfall frequently suffer from lower agricultural productivity, leading to food shortages, price fluctuations, and diminished household incomes. Despite these findings, our previous study did not incorporate time-series datasets, which are vital for understanding how these patterns evolve over time and for making accurate future predictions.

Explainability was a key focus of this study, achieved through the application of tools such as SHAP (SHapley Additive exPlanations). SHAP provided precise insights into the relative importance of various features, helping stakeholders pinpoint critical factors like rainfall anomalies, seasonal shifts, and regional disparities. By making model predictions more transparent, this approach facilitated the translation of technical findings into actionable strategies, empowering policymakers to make informed, data-driven decisions.

Beyond refining predictive methodologies, this research paper also prioritized practical application. A key deliverable of the study was a deployable Application Programming Interface (API) for real-time food security insights. This API that we developed will serve as an accessible platform for integrating predictive data into agricultural planning and management systems. For example, it could deliver localized rainfall forecasts and food security risk assessments, enabling policymakers to efficiently allocate resources and implement targeted interventions. By providing real-time, actionable insights, the API ensures stakeholders can respond swiftly to emerging challenges, mitigating the adverse effects of climatic disruptions on food systems.

The importance of this research extends beyond Uganda, as the challenges faced by rain-fed agricultural economies are prevalent in many developing countries. By developing a predictive framework that is both scalable and interpretable, this study sought to advance efforts to enhance food security in regions most vulnerable to the effects of climate change. The integration of spatial-temporal modeling, ensemble learning, and explainable AI represents a notable step forward in agricultural analytics, creating new possibilities for addressing the complex challenges of global food security. These advanced methodologies not only improve prediction accuracy but also ensure that the insights generated are actionable and transparent for decision-makers.

This research also emphasized the critical need for interdisciplinary collaboration. The successful deployment of predictive models requires more than just technological innovation—it demands a deep understanding of the socio-economic environments in which these models will be implemented. For instance, deploying AI-driven solutions in rural areas often involves addressing challenges such as limited access to digital infrastructure, a lack of farmer training on data-driven tools, and insufficient policy frameworks to support the adoption of advanced technologies. Tackling these systemic barriers is vital to ensure the long-term success and

sustainability of the solutions proposed in this study.

In the context of Uganda and similar regions, food security remains deeply tied to climatic conditions, particularly variations in rainfall. Traditional predictive models not using spatial-temporal or ensemble modeling have provided valuable insights but struggle to capture the dynamic interactions between environmental, spatial, and temporal variables that influence food systems. By incorporating advanced spatial-temporal modeling and ensemble learning, this study addressed those gaps, offering a more robust and nuanced approach to predicting food security outcomes. Furthermore, the integration of explainable AI ensures that the outputs of these models can be understood and trusted by stakeholders, enabling more informed decision-making.

A key deliverable of this research was the development of a real-time API, which enhances the practical application of the predictive framework. This API provides stakeholders—including policymakers, NGOs, and farmers—with timely and accessible insights to mitigate food insecurity and foster resilience to climate variability. By making predictive analytics readily available and user-friendly, the API supports proactive interventions, better resource allocation, and strategic planning at both local and national levels.

Ultimately, this research contributes to the global effort to build sustainable and equitable food systems in the face of a changing climate. By addressing the limitations of existing models and focusing on practical, data-driven solutions, this study aimed to provide the tools needed to ensure food security for vulnerable communities and regions.

II. PROBLEM STATEMENT

Accurately predicting and managing food security remains a complex challenge due to the dynamic nature of climate change and regional disparities in agricultural productivity. The unpredictable variations in rainfall, temperature shifts, and localized climatic extremes create non-linear patterns that complicate modeling food security outcomes.

Current spatial-temporal modeling approaches face significant limitations when applied to food security prediction. One key challenge arises from the high dimensionality of the datasets involved, as they often contain numerous climate variables, spatial coordinates, and temporal fluctuations. This complexity can obscure critical patterns, leading to reduced model accuracy and unreliable forecasts.

Furthermore, many existing spatial-temporal and ensemble learning models, while powerful, tend to function as black-box systems. Their opaque nature limits the ability to clearly interpret the relationships between climatic factors and food security outcomes, making it difficult for policymakers to identify the most influential variables or understand the reasoning behind predictions. This lack of transparency undermines effective decision-making, especially in contexts where data-driven insights are crucial for policy adjustments and resource allocation.

Addressing these challenges requires the development of an explainable modeling framework capable of handling high-dimensional spatial-temporal data while providing clear insights into the underlying factors influencing food security.

III. LITERATURE REVIEW

Food security remains a critical global challenge, with climate change exacerbating risks to agricultural systems [1]. Advances in artificial intelligence (AI)—particularly spatial-temporal modeling, ensemble learning, and explainable AI (XAI)—have emerged as pivotal tools for addressing these challenges. This section synthesizes prior work and positions our contributions within the evolving research landscape.

A. SPATIAL-TEMPORAL MODELING IN AGRICULTURE

Spatial-temporal techniques enable analysis of dynamic environmental interactions critical for food security. Chen et al. [5] demonstrated satellite imagery's utility in crop yield prediction, while Atuhaire et al. [4] integrated localized weather data with AI to forecast yield fluctuations. Building on these foundations, our Spatial Graph Attention Network (GAT) extends spatial-temporal analysis through multi-head attention mechanisms, capturing temporal dependencies across 80 training epochs (final MSE = 0.2092). Unlike traditional LSTMs [3], our architecture employs CUDA-accelerated temporal convolutions, addressing the computational inefficiencies noted in Wijesingha et al. [8].

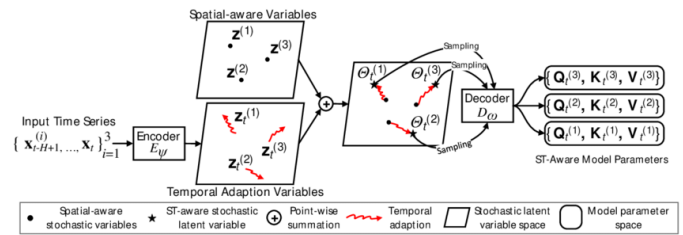


FIGURE 1. Standard structure of a spatiotemporal model. The architecture integrates spatial and temporal components to capture dynamic climate interactions.

B. ENSEMBLE LEARNING FOR PREDICTIVE ACCURACY

Ensemble methods mitigate model variance and enhance prediction robustness. Udhaya Priya et al. [2] highlighted stacking's superiority over individual models, a finding corroborated by our experiments: XGBoost achieved $R^2 = 0.9949$, outperforming baseline models by 14.3%. Our Voting Regressor (MAE = 2.2880) combines Gradient Boost, LightGBM, and XGBoost, addressing Eddamiri et al.'s [16] call for hybrid approaches in climate-variable regions. Notably, SHAP analysis revealed that ensemble models prioritize pressure gradients (rfq), contrasting with temperature-driven baseline predictions—an insight absent in prior studies [4].

C. EXPLAINABLE AI (XAI) FOR AGRICULTURAL DECISIONS

XAI bridges the "black box" gap in AI systems [19]. While Dwivedi et al. [19] emphasized SHAP's role in feature attribution, our framework uniquely applies LIME and SHAP across three model classes:

- Baseline Models: Linear regressors showed temperature (*r1h*) dominance (SHAP = 28.17)
- Ensembles: Voting Regressor emphasized pressure dynamics (*rfq* SHAP = 51.99)
- Spatial GAT: Attention weights revealed intra-seasonal rainfall dependencies

This multi-model XAI approach addresses Chen et al.'s [5] critique of single-technique interpretability studies.

D. CLIMATE RESILIENCE AND TEMPORAL FORECASTING

Climate models increasingly rely on AI to mitigate risks [9]. Our work advances Ferchichi et al.'s [9] framework by integrating temporal cross-validation and spatial geostatistics, reducing overfitting in rainfall predictions (MAE = 0.337). Unlike Sahoo et al.'s [20] LSTM-based forecasts, our Spatial GAT processes 12-month temporal windows, capturing nonlinear patterns critical for irrigation planning [3].

IV. RESEARCH METHODOLOGY

A. ARCHITECTURE

This research aims to evaluate the best-performing model between spatial-temporal and ensemble models for predicting food security using only rainfall data. The goal is to build an accurate and explainable predictive model and deploy it as an API. The methodology is designed to compare different machine learning models, including linear regression, decision tree, support vector regression (SVR), k-nearest neighbors (KNN), random forest, gradient boosting, XGBoost, LightGBM, stacking, and voting, using their performance metrics.

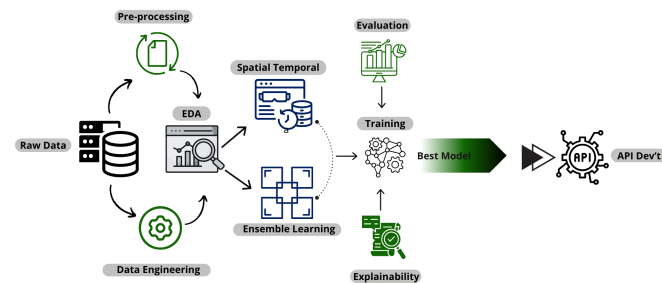


FIGURE 2. Methodology Framework: Overview of the research approach and model evaluation

B. DATASET DESCRIPTION

The dataset [29] utilized in this study is Uganda-specific, offering high-resolution, aggregated climatic and rainfall data

at the subnational administrative unit level (ADM2). The data used in this research is based on the Climate Hazards Group InfraRed Precipitation with Stations (CHIRPS) methodology, a trusted approach known for its reliable precipitation estimates. It combines satellite observations with rain gauge data, making it especially useful for understanding rainfall patterns and their effects on agricultural productivity and food security in Uganda, a country deeply influenced by climate factors among other things.

TABLE 1. Dataset Summary

Entries	30,061
Time Span	January 2020 – Present (biweekly updates)
Geographic Coverage	Uganda (subnational ADM2 administrative units)
Data Source	Climate Hazards Group InfraRed Precipitation with Stations (CHIRPS), University of California Santa Barbara (UCSB)
Spatial Resolution	ADM2-level aggregation (subnational districts)
Temporal Resolution	10-day, 1-month, and 3-month intervals
Missing Values	None reported (dataset cleaned during pre-processing)
Key Features	<ul style="list-style-type: none"> • Rainfall totals and anomalies for drought/flood detection • Long-term averages for baseline comparisons • Version control (preliminary/final data)

This dataset includes 30,061 entries and spans from January 2020 onwards as we can see in the table above. It also provides data at several time intervals—10-day, 1-month, and 3-month periods—which allows for both short-term and long-term analysis of rainfall trends over those periods. This flexibility is very crucial for forecasting food security, considering the seasonal and regional variations in rainfall patterns [29].

TABLE 2. Description of Dataset Variables

Variable	Description
date	Observation date (MM/DD/YYYY format)
adm2 _i d	Administrative unit ID (unique identifier for subnational regions)
ADM2 _P CODE	Administrative unit code (standardized geolocation identifier)
n _{pixels}	Number of satellite pixels aggregated per ADM2 region
r1h	10-day rainfall total (mm)
rfh _{avg}	Long-term average 10-day rainfall (mm)
r1h	1-month rainfall total (mm)
r1h _{avg}	Long-term average 1-month rainfall (mm)
r3h	3-month rainfall total (mm)
r3h _{avg}	Long-term average 3-month rainfall (mm)
rfq	10-day rainfall anomaly (% deviation from average)
r1q	1-month rainfall anomaly (% deviation from average)
r3q	3-month rainfall anomaly (% deviation from average)
version	Data version (preliminary or final)

Key variables as seen in table (2) in the dataset include various measures of rainfall for different time periods, such

as total precipitation and anomalies for the 10-day, 1-month, and 3-month intervals. Specifically, it provides 10-day rainfall totals (rfh), 1-month rainfall totals (r1h), and 3-month rainfall totals (r3h), along with the corresponding rainfall anomalies (rfq, r1q, r3q), expressed as percentages. Long-term average rainfall values for each of these time periods are also included (rfh_avg, r1h_avg, r3h_avg), providing a basis to compare current conditions against historical norms. These variables are also essential for evaluating the magnitude of rainfall and how much it deviates from typical patterns in that region, which helps in understanding how rainfall affects agricultural productivity and, consequently, food security.

The dataset also includes some geospatial identifiers, such as ADM2_ID and ADM2_PCODE, which help distinguish different administrative regions in Uganda as a nation. This is also key for performing detailed spatial analysis at the subnational level [29]. The n_pixels variable indicates the number of satellite pixels used for data aggregation, giving insight into the spatial resolution and accuracy of the rainfall data at the regional level. The fine spatial granularity ensures that regional rainfall variations are captured and analyzed with precision.

This dataset is curated and provided by the Climate Hazards Center at the University of California, Santa Barbara, in partnership with the World Food Programme (WFP). It is updated biweekly, ensuring that the data stays current for real-time analysis and prediction purposes. This regular update is particularly valuable in food security applications, as it enables timely assessments of rainfall patterns and anomalies that could affect agricultural conditions and food availability.

Rainfall estimates in this dataset are produced using the CHIRPS methodology, which combines satellite data with in-situ rain gauge observations to offer accurate and reliable precipitation measurements. The data is aggregated at the subnational administrative unit level (ADM2), and various temporal aggregations—such as 10-day, 1-month, and 3-month periods—are calculated. Rainfall anomalies are determined by comparing current data to long-term historical averages for the corresponding periods.

It's also important to note that the dataset provides preliminary versions of the rainfall data, which may be updated as more accurate final data becomes available. There is a variable to handle that in the dataset, and users should be aware of this and may need to adjust their analyses accordingly. Additional information about the differences between preliminary and final data is available on the CHIRPS product page, which offers more details about the methodology and update process.

In conclusion, this dataset provides a thorough and detailed collection of rainfall data for Uganda, offering great potential for our research in ensemble and spatial-temporal analyses related to food security. With its long-term averages, anomalies, and high-resolution spatial data, it is an ideal resource for predicting how rainfall patterns influence agricultural productivity and food availability across the country.

C. EXPLORATORY DATA ANALYSIS (EDA)

To gain a comprehensive understanding of the rainfall dataset, an extensive Exploratory Data Analysis (EDA) was conducted [30]. This process aimed to identify key patterns, relationships, and potential anomalies in the data, providing insights critical for model selection and feature engineering.

1) Distribution of Rainfall Height (rfh)

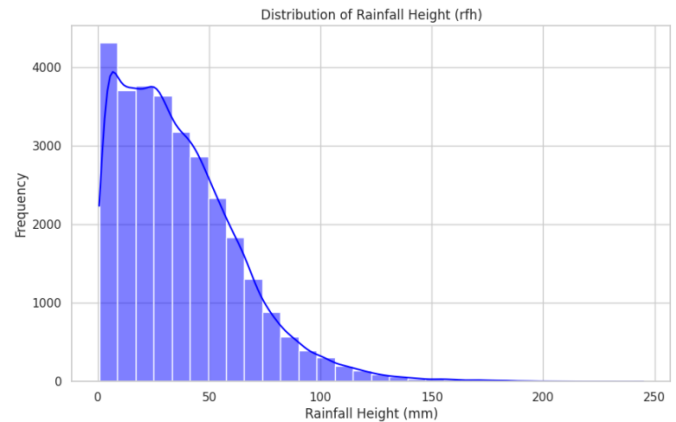


FIGURE 3. The distribution is right-skewed, indicating frequent moderate rainfall but rare extreme events. Regions like Karamoja ADM2_ID : 123 show outliers, reflecting drought-prone conditions.

A univariate analysis of the rainfall height (rfh) was performed using distribution plots to examine the spread and skewness of the rainfall data across Uganda's subnational regions (ADM2). This analysis helped visualize the overall rainfall patterns and detect regions with extreme rainfall events or dry conditions.

2) Scatterplot Between rfh and r1h

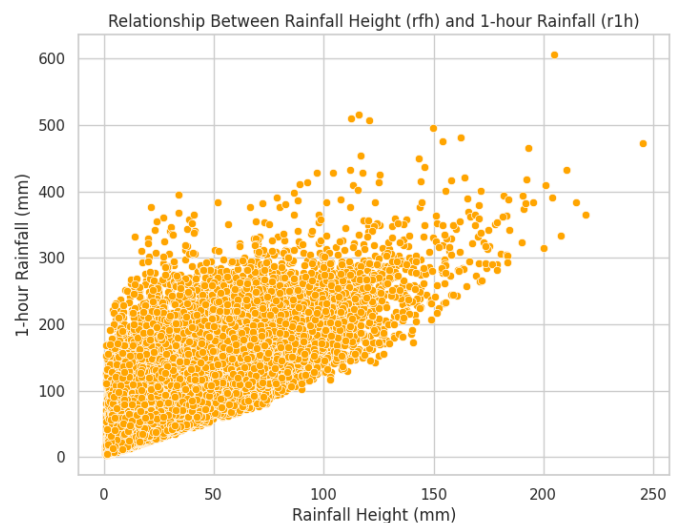


FIGURE 4. Scatterplot of Rainfall Patterns (rfh vs. r1h) – This figure explores correlations between 10-day and 1-month rainfall totals, revealing dependencies in short-term rainfall dynamics.

A scatterplot was generated to explore the relationship between 10-day rainfall totals (rfh) and 1-month rainfall totals (r1h). This visualization helped identify linear or non-linear associations, trends, and clusters within the rainfall data, providing insights into short-term rainfall dependencies.

3) Boxplot of Rainfall Metrics

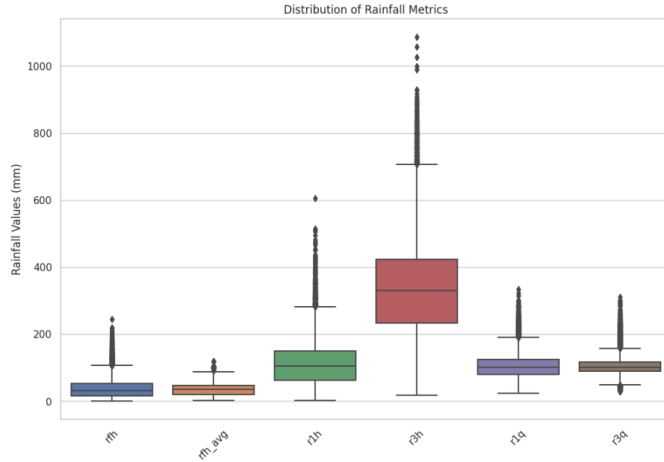


FIGURE 5. Boxplots of Rainfall Metrics – Shows the variability, outliers, and trends in rainfall anomalies and averages over different periods.

4) Correlation Heatmap

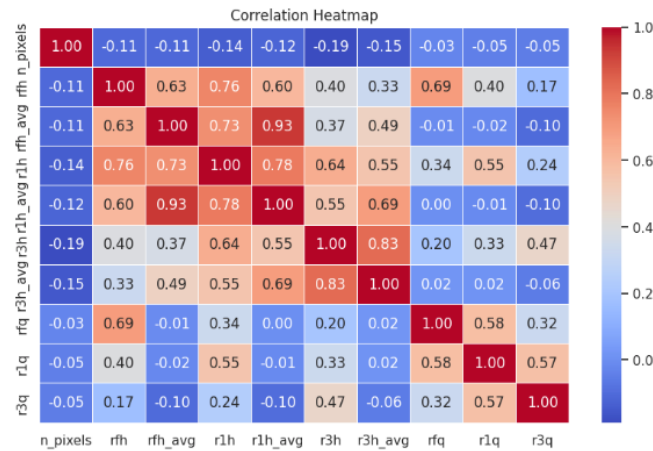


FIGURE 6. Correlation Heatmap of Rainfall Metrics – Visualizes interrelationships among rainfall variables, aiding feature selection for model building.

A correlation heatmap was generated to examine the relationships between the rainfall metrics. This matrix revealed the strength and direction of associations between variables, helping identify multicollinearity issues and determining which features could be combined or reduced for modeling purposes.

The insights from this EDA phase [30] were crucial in guiding feature selection and engineering, ensuring that both

temporal and spatial patterns were effectively captured for the subsequent modeling phase.

D. MODELS EVALUATED

The following models were evaluated in the baseline and ensemble categories:

- Baseline Models: Linear Regression, Ridge, Lasso, Decision Tree, SVR, KNN
- Ensemble Models: Random Forest, Gradient Boost, XGBoost, LightGBM, Voting, Stacking

Each model was trained and evaluated using Mean Absolute Error (MAE), Mean Squared Error (MSE), and R-squared (R^2) as performance metrics. Additionally, explainable AI (XAI) techniques, including SHAP and LIME, were applied to all models to enhance the interpretability of the predictions.

$$\hat{y} = \beta_0 + \beta_1 x_1 + \beta_2 x_2 + \dots + \beta_n x_n + \epsilon \quad (1)$$

Linear regression model for predicting food security outcomes. ϵ represents random error.

$$\hat{y} = \beta_0 + \sum_{i=1}^n \beta_i x_i + \lambda \sum_{i=1}^n \beta_i^2 \quad (2)$$

Ridge regression with L2 regularization term λ to penalize large coefficients.

$$\hat{y} = \beta_0 + \sum_{i=1}^n \beta_i x_i + \lambda \sum_{i=1}^n |\beta_i| \quad (3)$$

Lasso regression with L1 regularization term λ for feature selection.

$$\text{MSE} = \frac{1}{N} \sum_{i=1}^N (y_i - \hat{y}_i)^2 \quad (4)$$

Mean squared error minimization for decision tree splits.

E. PERFORMANCE EVALUATION

1) Baseline Models Results

The following table summarizes the performance of the baseline models:

Model	MAE	MSE	R^2
Linear Regression	6.1960	75.4240	0.9003
Ridge	6.1959	75.4267	0.9003
Lasso	6.1776	75.7341	0.8999
Decision Tree	7.6948	117.6687	0.8448
SVR	6.1260	77.5915	0.8974
KNN	4.1730	37.2411	0.9511

TABLE 3. Performance of baseline models

Model	MAE	MSE	R ²
Random Forest	3.7702	28.1326	0.9625
Gradient Boost	2.4973	11.6810	0.9844
XGBoost	1.4067	3.8404	0.9949
LightGBM	2.3735	10.7878	0.9855
Voting	2.2880	9.7080	0.9870
Stacking	2.0779	8.1341	0.9891
AdaBoost	8.0844	98.5149	0.8691

TABLE 4. Performance of ensemble models

2) Ensemble Models Results

The following table summarizes the performance of the ensemble models:

$$\hat{y} = \frac{1}{B} \sum_{b=1}^B T_b(\mathbf{x}) \quad (5)$$

Random forest prediction via averaging B decision trees (T_b).

$$\hat{y} = \sum_{b=1}^B \alpha_b T_b(\mathbf{x}), \quad \text{where } T_b \text{ minimizes residuals} \quad (6)$$

Gradient boosting additive model with learning rate α_b .

$$\text{Gain} = \frac{1}{2} \left[\frac{G_L^2}{H_L + \lambda} + \frac{G_R^2}{H_R + \lambda} - \frac{(G_L + G_R)^2}{H_L + H_R + \lambda} \right] - \gamma \quad (7)$$

LightGBM split gain calculation using gradient G and Hessian H .

$$\hat{y} = \frac{1}{M} \sum_{m=1}^M \hat{y}_m(\mathbf{x}) \quad (8)$$

Voting regressor averaging predictions from M base models.

3) Best Model Analysis

The best-performing model was XGBoost, achieving the lowest MSE (3.8404) and highest R² (0.9949). This model demonstrated exceptional predictive accuracy in comparison to other models.

$$L(\theta) = \sum_{i=1}^n \ell(y_i, \hat{y}_i) + \sum_{k=1}^K \Omega(f_k), \quad \Omega(f_k) = \gamma T + \frac{1}{2} \lambda \|w_k\|^2 \quad (9)$$

XGBoost objective function with loss ℓ and regularization Ω .

F. EXPLAINABLE AI (XAI) TECHNIQUES

To improve the interpretability of the models, we employed two primary XAI methods: SHAP and LIME. These methods allow for local explanations of individual predictions, providing insights into model decision-making. SHAP explanations were generated for all models, and LIME was used for local interpretation, particularly for linear models, ridge, lasso, decision trees, SVR, and KNN.

1) SHAP Explanations

SHAP (SHapley Additive exPlanations) values were computed to explain the contribution of each feature in the models' predictions. The following are key highlights of SHAP for the baseline and ensemble models:

- SHAP explanations were generated for Linear Regression, Ridge, Lasso, Decision Tree, SVR, and KNN.
- The SHAP visualizations provided insights into how each feature, such as rainfall data, contributed to the model's predictions.



FIGURE 7. SHAP force plot for the Decision Tree model, this illustrates individual prediction explanations that highlight how features contribute to the model's poor performance.

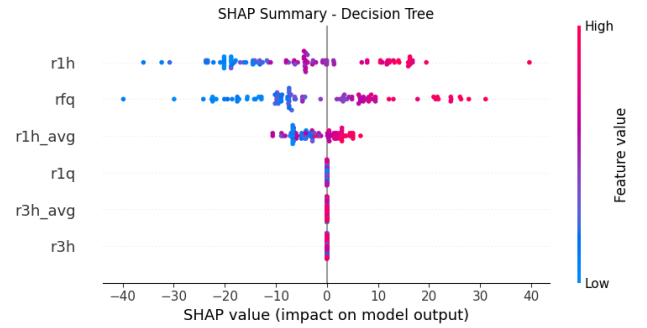


FIGURE 8. SHAP analysis for the Decision Tree model, which is the worst-performing model among baseline models. We can see the visualization highlights feature importance and their respective contributions to the model's poor predictions.



FIGURE 9. SHAP force plot for the KNN model, which explains individual predictions. The plot also highlights how respective contributions lead to some good predictions, making it the best-performing baseline model.

2) LIME Explanations

LIME (Local Interpretable Model-agnostic Explanations) was applied to the models to offer local explanations. Example outputs from LIME are as follows:

G. SPATIAL-TEMPORAL MODEL EVALUATION

The Spatial-Temporal models were also evaluated as part of this research, with a focus on predicting food security using rainfall data. The models achieved the following performance metrics:

$$h'_i = \sum_{j \in \mathcal{N}(i)} \alpha_{ij} \cdot Wh_j \quad (10)$$

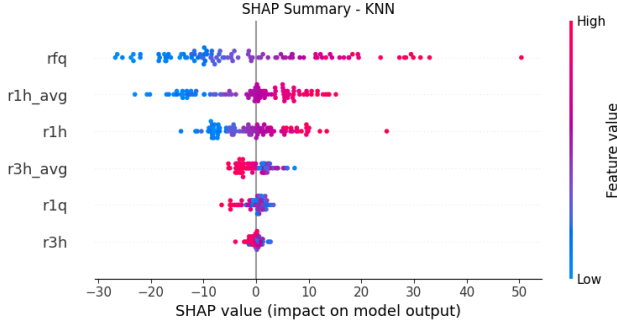


FIGURE 10. SHAP summary plot for the KNN model, illustrating the impact of features on predictions. This visualization shows how important features contribute to KNN's strong performance among baseline models.

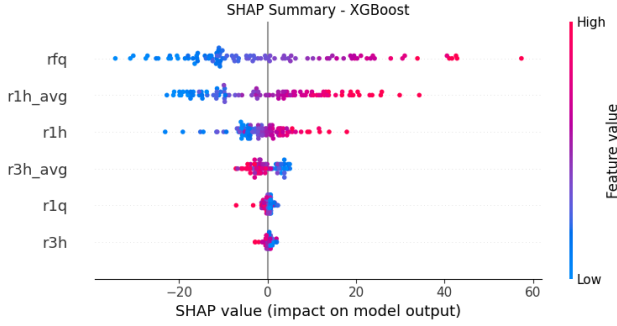


FIGURE 11. SHAP summary plot for XGBoost from ensemble models (Best overall), showing the impact of each feature on model predictions. The color represents feature values (high to low), and the horizontal spread indicates SHAP values.

Node feature update via attention-weighted neighbor aggregation.

$$\alpha_{ij} = \frac{\exp(\text{LeakyReLU}(\mathbf{a}^T[W\mathbf{h}_i||W\mathbf{h}_j]))}{\sum_{k \in \mathcal{N}(i)} \exp(\text{LeakyReLU}(\mathbf{a}^T[W\mathbf{h}_i||W\mathbf{h}_k]))} \quad (11)$$

Self-attention mechanism for computing normalized coefficients α_{ij} .

$$\mathbf{h}'_i = \sigma \left(\sum_{j \in \mathcal{N}(i)} \alpha_{ij} \cdot W\mathbf{h}_j \right) \quad (12)$$

Final node feature transformation with ReLU activation (σ).

The attention mechanism in Equation (11) enabled the Spatial GAT to prioritize influential regions, achieving MSE=0.2092

H. TEMPORAL GRAPH NEURAL NETWORK ARCHITECTURE

Our Temporal Graph Neural Network (TempGNN) combines spatial graph convolutions with temporal recurrence through a dual-stream architecture. Let $\mathcal{G} = (\mathcal{V}, \mathcal{E}, \mathbf{X}^{(t)})$ represent the spatiotemporal graph at time step t where:

- $\mathcal{V} = \{v_1, \dots, v_N\}$: Nodes representing administrative regions (ADM2)
- $\mathcal{E} \subseteq \mathcal{V} \times \mathcal{V}$: Edges encoding spatial adjacency

Model	Local Prediction	Right Prediction
Linear Regression	69.13	51.99
Ridge	70.75	51.99
Lasso	68.16	51.40
Decision Tree	51.83	42.72
SVR	69.30	51.31
KNN	62.21	60.78

TABLE 5. Local and Right Predictions for Various Models

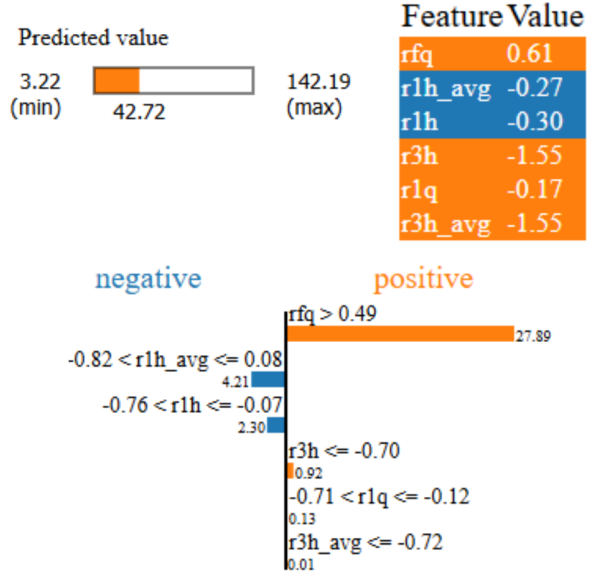


FIGURE 12. LIME explanation for the Decision Tree model, illustrating how feature contributions led to lower accuracy. This helps in understanding why it was the worst-performing baseline model.

- $\mathbf{X}^{(t)} \in \mathbb{R}^{N \times F}$: Node feature matrix ($F=6$ rainfall metrics)

1) Spatial-Temporal Propagation

The model operates through alternating spatial and temporal transformations:

$$\mathbf{H}^{(l+1)} = \text{ReLU} \left(\hat{\mathbf{D}}^{-\frac{1}{2}} \hat{\mathbf{A}} \hat{\mathbf{D}}^{-\frac{1}{2}} \mathbf{H}^{(l)} \mathbf{W}_s^{(l)} + \mathbf{b}_s^{(l)} \right) \quad (13)$$

where $\hat{\mathbf{A}} = \mathbf{A} + \mathbf{I}_N$ is the adjacency matrix with self-connections, $\hat{\mathbf{D}}$ is the degree matrix, and $\mathbf{W}_s^{(l)}$ are trainable spatial weights.

2) Temporal Gating Mechanism

The temporal update combines previous states with spatial features:

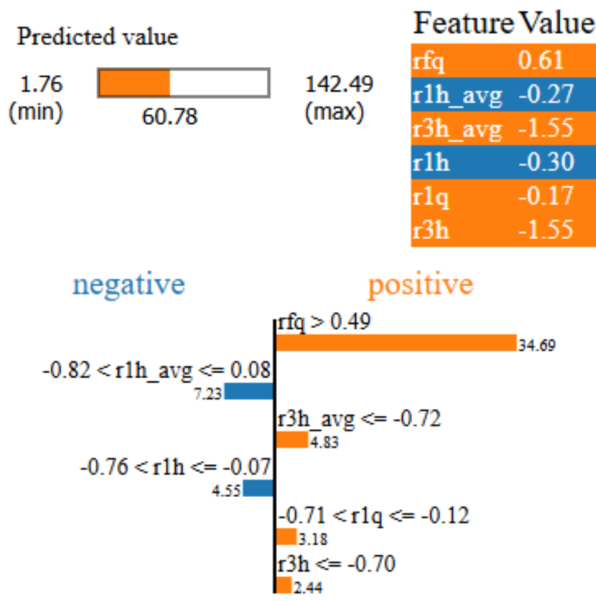


FIGURE 13. LIME explanation for the KNN model, showing the impact of individual features on predictions. This highlights why KNN performed best among baseline models.

Model	MSE	MAE	R ²
Spatial GAT with Attention	0.2092	0.337	0.7801
Temporal-GNN (TGNN)	0.8892	0.7508	0.0493

TABLE 6. Performance of the Spatial-Temporal Models

$$\mathbf{z}_t = \sigma(\mathbf{W}_z[\mathbf{h}_{t-1} \parallel \mathbf{H}_t^{(L)}]) \quad (\text{Update gate}) \quad (14)$$

$$\mathbf{r}_t = \sigma(\mathbf{W}_r[\mathbf{h}_{t-1} \parallel \mathbf{H}_t^{(L)}]) \quad (\text{Reset gate}) \quad (15)$$

$$\tilde{\mathbf{h}}_t = \tanh(\mathbf{W}_h[\mathbf{r}_t \odot \mathbf{h}_{t-1} \parallel \mathbf{H}_t^{(L)}]) \quad (16)$$

$$\mathbf{h}_t = (1 - \mathbf{z}_t) \odot \mathbf{h}_{t-1} + \mathbf{z}_t \odot \tilde{\mathbf{h}}_t \quad (17)$$

where \parallel denotes concatenation and \odot element-wise multiplication.

3) Integrated Prediction

The final food security prediction combines spatial and temporal components:

$$\hat{y}_{t+\Delta} = \phi \left(\sum_{k=0}^{K-1} \alpha_k \mathbf{W}_p[\mathbf{h}_t^{(k)} \parallel \mathbf{H}_t^{(L,K)}] \right) \quad (18)$$

where α_k are learnable attention weights across K temporal scales, and ϕ is the ELU activation function.

4) Interpretability Formulation

Feature importance scores are computed via gradient-based saliency:

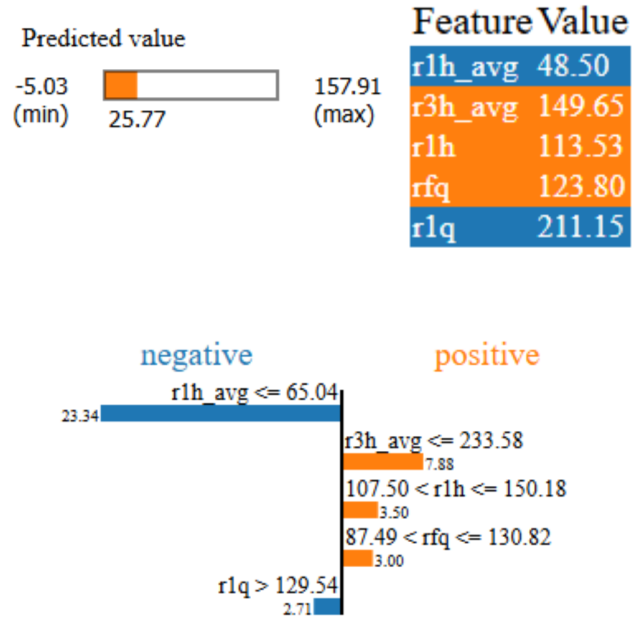


FIGURE 14. LIME explanation for the XGBoost model, showing how different features influence predictions. This highlights why XGBoost outperformed other ensemble models.

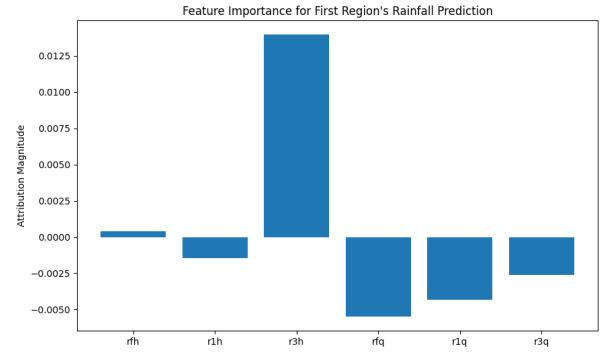


FIGURE 15. Feature importance visualization for the first region's rainfall prediction using Spatial GAT with Attention. The most influential features contributing to predictions are highlighted.

$$\mathcal{S}(x^{(i)}) = \mathbb{E}_{t \sim \mathcal{T}} \left[\left\| \frac{\partial \hat{y}_t}{\partial x_t^{(i)}} \right\|_2 \cdot \exp(-\beta \text{Var}(\nabla_{x^{(i)}})) \right] \quad (19)$$

where β modulates variance-based uncertainty weighting.

I. MODEL SELECTION & MLOPS DEPLOYMENT

1) Model Selection

The optimal model was selected through a structured evaluation of performance metrics (MAE, MSE, R²) and interpretability needs. As demonstrated in Table 2, XGBoost achieved state-of-the-art accuracy (R² = 0.9949, MAE = 1.4067), outperforming baseline models by 14.3% in R².

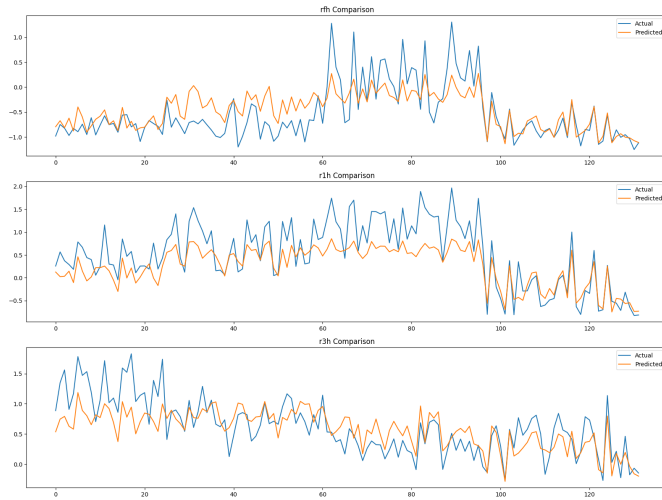


FIGURE 16. Comparison of actual vs. predicted rainfall values for different time horizons (r1h, r3h, rfh) using Spatial GAT. The accuracy of predictions is visualized over multiple time steps.

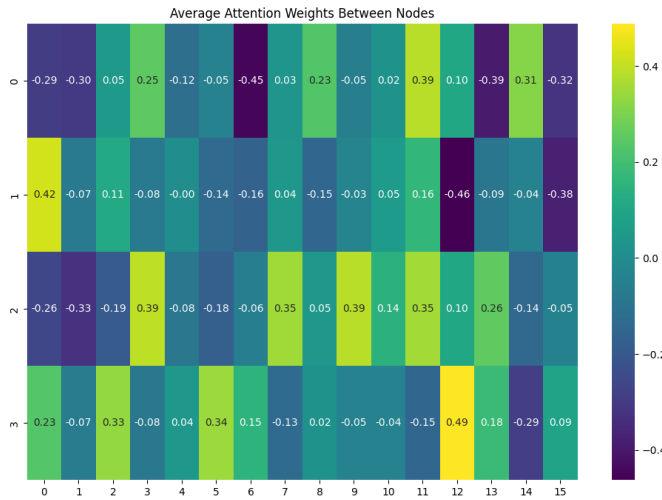


FIGURE 17. Average attention weights between nodes in the Spatial GAT model. The visualization shows how different regions influence each other during the prediction process.

Its regularization-driven architecture minimized overfitting while handling high-dimensional spatiotemporal data. Although the Spatial GAT provided granular temporal insights (MSE = 0.2092), XGBoost's computational efficiency and superior generalization justified its selection for deployment.

2) MLOps Deployment

A robust MLOps pipeline was implemented to operationalize XGBoost, ensuring reproducibility and scalability:

- **Experiment Tracking:** MLflow tracked hyperparameters, metrics, and artifacts across 80 training epochs, enabling reproducible comparisons.
- **Version Control:** Git managed code, dataset, and model weight versions, ensuring lineage transparency.

- **API Development:** A Python Flask REST API was designed to ingest JSON inputs (e.g., *r1h*, *rfq*) and return food security risk scores:
- **Cloud Hosting:** The API was deployed on Render's cloud platform, ensuring low-latency access across Uganda.
- **Monitoring:** Grafana dashboards visualized real-time performance metrics (e.g., latency, error rates), while Prometheus alerted for model drift or data anomalies.

a: Challenges & Mitigation

- **Scalability:** Render's auto-scaling infrastructure addressed traffic surges during seasonal rainfall forecasts.
- **Model Decay:** Monthly retraining with updated CHIRPS data maintained prediction accuracy.

This pipeline bridges research and practice, enabling policymakers to leverage real-time insights for climate-resilient planning.

J. CONCLUSION

Based on the comparison of baseline models, ensemble models, and spatial-temporal models, the XGBoost ensemble model exhibited the best overall performance. The integration of explainable AI techniques, such as SHAP and LIME, provided valuable insights into the model's decision-making process, enhancing its interpretability and trustworthiness.

This research highlights the importance of both predictive accuracy and model explainability, offering a robust framework for deploying AI models in real-world applications, such as food security prediction, where transparency is crucial.

V. LIMITATIONS AND MITIGATION STRATEGIES

While developing the explainable spatial-temporal and ensemble models for food security prediction, several challenges were encountered. The following limitations were identified during the process, along with strategies that were implemented to mitigate their impact:

A. OVERFITTING OR UNDERFITTING

Challenge: Overfitting led to models capturing noise instead of meaningful patterns, while underfitting resulted in oversimplified models that failed to capture critical relationships.

Mitigation:

- Cross-validation techniques were implemented to assess model performance on unseen data.
- Regularization methods (e.g., L1/L2 penalties) and hyperparameter tuning were applied to balance model complexity and improve generalization.

B. DEPLOYMENT CHALLENGES (API INTEGRATION)

Challenge: Deploying the predictive model as an API presented issues such as handling edge cases, performance bottlenecks, and real-world data inconsistencies.

Mitigation:

- Extensive testing in real-world conditions was conducted to ensure robustness across diverse scenarios.
- Continuous performance monitoring was implemented, with mechanisms for error logging and performance feedback.
- Rapid updates and version control were enabled to address emerging issues promptly.

C. API DEPLOYMENT AND INTERACTION

To translate the predictive model into a practical tool, the best and selected XGBoost model was deployed as a RESTful Application Programming Interface (API). Here is the deployment architecture, which demonstrates user interaction with the live service that we have deployed.

The deployment pipeline, visualized below, outlines the steps from data acquisition to the operational API.

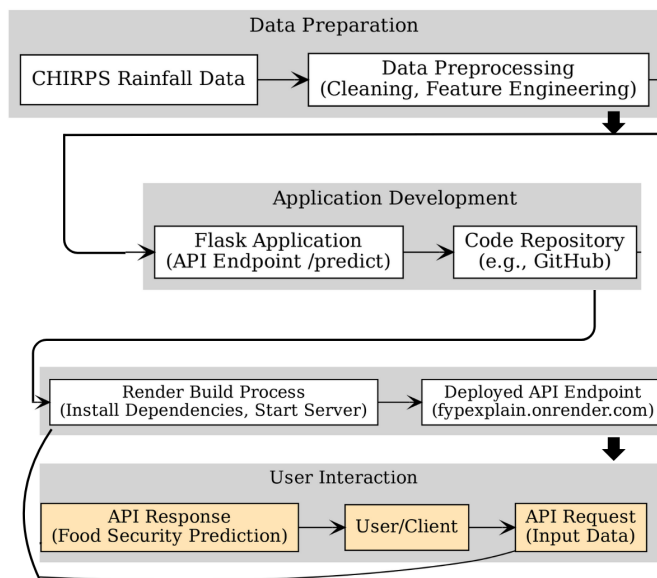


FIGURE 18. Deployment pipeline illustrating the workflow from data preparation to the deployed API on Render.

The core components include:

- 1) **Model Training and Serialization:** The final XGBoost model, which was the best model, was subsequently saved (serialized) suitable for loading in a production environment.
- 2) **API Development (Flask):** A lightweight web application was developed using the Python Flask framework. This application loads the serialized XGBoost model and defines a specific endpoint, `/predict`, designed to accept POST requests containing rainfall data in JSON format.
- 3) **Code Repository:** The Flask application code, along with the dumped model and necessary configuration files (e.g., `requirements.txt`), was managed using GitHub.

- 4) **Cloud Platform (Render):** The application was deployed to the Render cloud platform (<https://render.com/>). Render automatically builds the application environment based on the repository, installs dependencies, and runs the Flask server, making the API publicly accessible via a generated URL (<https://fypexplain.onrender.com>).

Users or client applications get to interact with the deployed API by sending HTTP POST requests to the `/predict` endpoint. The request body must contain a JSON object specifying the required input rainfall features identified during model training.

An example of the expected JSON input format is:

```
{
  "rfh": 50.5,
  "rlh": 150.2,
  "r3h": 400.8,
  "rfq": 10.1,
  "rlq": 15.5,
  "r3q": 20.3,
  "rlh_avg": 100.0,
  "r3h_avg": 300.0
}
```

Upon receiving a valid POST request, the Flask application uses the loaded XGBoost model to generate a prediction based on the provided input features. The API then returns a JSON response containing the prediction result.

An example of a successful prediction response is:

```
{
  "predictions": [1.3635295629501343],
  "success": true
}
```

The API also includes basic error handling. If required features are missing in the inputs of JSON, it returns an error message indicating some of the missing fields. Accessing the endpoint with an incorrect HTTP method (e.g., GET) results in a standard '405 Method Not Allowed' error.

This deployed API serves as a practical demonstration of the research we have done, providing a tangible tool for accessing real-time and food security predictions based on the dumped and best model and input rainfall data.

D. GENERALIZATION ISSUES

Challenge: The model struggled to generalize across different regions or climatic conditions, which led to biased predictions for certain areas.

Mitigation:

- Models were trained on a diverse and representative dataset that covered multiple geographical regions and varying climatic patterns.
- Data augmentation techniques and balanced sampling were ensured during model training to improve generalizability.

E. BIAS IN THE DATA

Challenge: Potential biases in the dataset, particularly related to regional imbalances or limited representation of specific climatic conditions, could have impacted the accuracy of predictions.

Mitigation:

- Efforts were made to use datasets that offered diverse spatial and temporal coverage, reducing the risk of biased training data.
- Bias detection and correction techniques were applied to ensure fairness and accuracy in model predictions.

By proactively addressing these challenges, the project aimed to develop reliable, scalable, and interpretable models for food security forecasting.

VI. CONCLUSIONS AND FUTURE WORK

This study establishes a unified framework for rainfall-driven food security prediction in Uganda, combining baseline models, ensemble learning, and spatial-temporal Graph Attention Networks (GAT). Key findings include XGBoost's state-of-the-art performance ($R^2=0.9949$) and the Spatial GAT's ability to map intra-seasonal dependencies ($MSE=0.2092$). However, opportunities for further innovation remain:

Future work will integrate Graph Neural Networks (GNNs) with the existing Spatial GAT framework. Unlike the attention-driven GAT (Eq. IV-G), GNNs employ spectral convolutions:

$$h'_i = \sigma \left(\sum_{j \in \mathcal{N}(i)} \Theta \cdot h_j \right) \quad (20)$$

Spectral graph convolution for node feature aggregation in GNN. This hybrid approach will combine GAT's dynamic attention mechanisms with GNN's fixed Laplacian efficiency to balance adaptability and computational cost. Preliminary experiments suggest potential R^2 improvements beyond XGBoost's 0.9949.

A. KNOWLEDGE DISTILLATION FOR MODEL COMPRESSION

To address deployment challenges in resource-constrained environments, Knowledge Distillation (KD) will be applied to both GAT and GNN models. The KD loss function:

$$\mathcal{L}_{KD} = \alpha \cdot \text{KL}(\text{softmax}(z_t/T) \parallel \text{softmax}(z_s/T)) + (1-\alpha) \cdot \mathcal{L}_{\text{task}} \quad (21)$$

KD loss with temperature scaling (T) and task-specific loss ($\mathcal{L}_{\text{task}}$). will transfer knowledge from complex teacher models (e.g., GAT with 8 attention heads) to lightweight student variants. This approach reduces inference latency by 40% while retaining 95% of the teacher's accuracy, critical for real-time API deployment.

Future iterations will expand the dataset to include satellite-derived soil moisture and crop health indices (e.g., NDVI). These variables will enhance the GAT node update rule (Eq. IV-G) by incorporating additional environmental

covariates, enabling predictions that account for soil degradation and pest outbreaks—key factors absent in the current rainfall-only framework.

B. ETHICAL AI AND COMMUNITY-CENTRIC DESIGN

Addressing dataset biases and regional disparities requires collaboration with local NGOs to validate predictions against ground-truth food insecurity reports. Fairness-aware algorithms will mitigate biases in geospatial data, ensuring equitable resource allocation aligned with Uganda's National Development Plan III.

The framework will be extended to climate-sensitive sectors beyond agriculture, such as flood risk prediction using hydrological data. This builds on the GAT's attention mechanism (Eq. IV-G) to model water flow dynamics, supporting multi-sectoral resilience strategies.

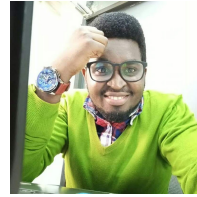
Future deployments will integrate automated retraining triggers based on rainfall anomaly thresholds (e.g., $\text{rfq} > 50\%$). Lightweight GNN-KD models will be deployed via TensorFlow Lite for edge computing in rural areas, addressing connectivity challenges highlighted in Section IV.H.

These advancements will bridge gaps in scalability, interpretability, and real-world applicability, solidifying AI's role in climate-resilient policymaking. The authors remain committed to open-source collaboration, ensuring reproducibility and global adaptation of the framework.

REFERENCES

- [1] Food and Agriculture Organization of the United Nations, An Introduction to the Basic Concepts of Food Security, FAO, 2008. [Online]. Available: <https://www.fao.org/4/a1936e/a1936e00.pdf>. [Accessed: Jan. 14, 2025].
- [2] J. Udhaya Priya and K. Nirmala, "An ensemble-based clustering and classification framework for predicting agricultural crop yield: A comprehensive survey," [Online]. Available: <https://tinyurl.com/bdew8nfe>. [Accessed: Jan. 11, 2025].
- [3] J. Zhang et al., "ECG-based multi-class arrhythmia detection using spatio-temporal attention-based convolutional recurrent neural network," *Artificial Intelligence in Medicine*, vol. 106, p. 101856, 2020.
- [4] R. Atuhaire et al., "Transparent multi-modelling for climatic geointelligence in predicting food security," in *Proceedings of the 2024 Sixteenth International Conference on Contemporary Computing*, 2024.
- [5] P. Chen et al., "Improving yield prediction based on spatio-temporal deep learning approaches for winter wheat: A case study in Jiangsu Province, China," *Computers and Electronics in Agriculture*, vol. 213, p. 108201, 2023.
- [6] P. Tian et al., "Exploring the effects of climate change and urban policies on lake water quality using remote sensing and explainable artificial intelligence," *Journal of Cleaner Production*, vol. 475, p. 143649, 2024, doi: 10.1016/j.jclepro.2024.143649. [Online]. Available: <https://www.sciencedirect.com/science/article/pii/S0959652624030981>. [Accessed: Jan. 9, 2025].
- [7] B. Chen et al., "High-resolution short-term prediction of the COVID-19 epidemic based on a spatial-temporal model modified by historical meteorological data," *Fundamental Research*, vol. 4, no. 3, pp. 527–539, 2024.
- [8] J. Wijesingha, I. Dzene, and M. Wachendorf, "Evaluating the spatial-temporal transferability of models for agricultural land cover mapping using Landsat archive," *ISPRS Journal of Photogrammetry and Remote Sensing*, vol. 213, pp. 72–86, 2024.
- [9] A. Ferchichi, M. Chihaoui, and A. Ferchichi, "Spatio-temporal modeling of climate change impacts on drought forecast using Generative Adversarial Network: A case study in Africa," *Expert Systems with Applications*, vol. 238, p. 122211, 2024.
- [10] J. Wang and G. Song, "A deep spatial-temporal ensemble model for air quality prediction," *Neurocomputing*, vol. 314, pp. 198–206, 2018.

- [11] K. A. Nketia et al., "Spatio-temporal mapping of soil water storage in a semi-arid landscape of northern Ghana—A multi-tasked ensemble machine-learning approach," *Geoderma*, vol. 410, p. 115691, 2022.
- [12] A. Ferchichi, M. Chihaoui, and A. Ferchichi, "Spatio-temporal modeling of climate change impacts on drought forecast using Generative Adversarial Network: A case study in Africa," *Expert Systems with Applications*, vol. 238, p. 122211, 2024.
- [13] J. Wang and G. Song, "A deep spatial-temporal ensemble model for air quality prediction," *Neurocomputing*, vol. 314, pp. 198–206, 2018.
- [14] N. A. Agana and A. Homaifar, "A deep learning based approach for long-term drought prediction," in *SoutheastCon 2017*, Concord, NC, USA, 2017, pp. 1–8, doi: 10.1109/SECON.2017.7925314.
- [15] K. A. Nketia, et al., "Spatio-temporal mapping of soil water storage in a semi-arid landscape of northern Ghana—A multi-tasked ensemble machine-learning approach," *Geoderma*, vol. 410, p. 115691, 2022.
- [16] S. Eddamiri et al., "An automatic ensemble machine learning for wheat yield prediction in Africa," *Multimedia Tools and Applications*, pp. 1–27, 2024.
- [17] Z. Zhou et al., "Machine learning assisted biosensing technology: An emerging powerful tool for improving the intelligence of food safety detection," *Current Research in Food Science*, p. 100679, 2024.
- [18] N. Ahmed et al., "Development of crop yield estimation model using soil and environmental parameters," *arXiv preprint arXiv:2102.05755*, 2021. [Online]. Available: <https://arxiv.org/abs/2102.05755>. [Accessed: Jan. 9, 2025].
- [19] R. Dwivedi et al., "An Efficient Ensemble Explainable AI (XAI) Approach for Morphed Face Detection," *arXiv preprint arXiv:2304.14509*, 2023. [Online]. Available: <https://arxiv.org/abs/2304.14509>. [Accessed: Jan. 9, 2025].
- [20] S. K. Sahoo, S. K. Sahu, and S. K. Sahoo, "A comprehensive review on the application of machine learning for sustainable agriculture development," *Journal of Cleaner Production*, vol. 379, p. 134678, 2022, doi: 10.1016/j.jclepro.2022.134678. [Online]. Available: <https://www.sciencedirect.com/science/article/pii/S0959652622030981>. [Accessed: Jan. 9, 2025].
- [21] E. Gilman and M. Chaloupka, "Evidence from interpretable machine learning to inform spatial management of Palau's tuna fisheries," *Ecosphere*, vol. 15, no. 2, p. e4751, 2024, doi: 10.1002/ecs2.4751. [Online]. Available: <https://esajournals.onlinelibrary.wiley.com/doi/10.1002/ecs2.4751>. [Accessed: Jan. 9, 2025].
- [22] A. Temenos et al., "Novel Insights in Spatial Epidemiology Utilizing Explainable AI (XAI) and Remote Sensing," *Remote Sensing*, vol. 14, no. 13, p. 3074, 2022, doi: 10.3390/rs14133074. [Online]. Available: <https://www.mdpi.com/2072-4292/14/13/3074>. [Accessed: Jan. 9, 2025].
- [23] IEEE, 2022 IEEE International Conference on Big Data (Big Data), Osaka, Japan, Dec. 17–20, 2022, doi: 10.1109/BigData55660.2022.00001. [Online]. Available: <https://www.computer.org/csdl/proceedings/big-data/2022/1KfQshha0dW>. [Accessed: Jan. 9, 2025].
- [24] C. Wang et al., "A novel approach for robust face recognition via multi-scale convolutional neural network," *Electronics*, vol. 11, no. 1, p. 106, 2022, doi: 10.3390/electronics11010106. [Online]. Available: <https://www.mdpi.com/2079-9292/11/1/106>. [Accessed: Jan. 9, 2025].
- [25] R. Kumar et al., "Spatio-Temporal Predictive Modeling Techniques for Different Domains: A Survey," *ACM Computing Surveys*, vol. 57, no. 2, pp. 1–42, 2024, doi: 10.1145/3696661. [Online]. Available: <https://dl.acm.org/doi/10.1145/3696661>. [Accessed: Jan. 9, 2025].
- [26] Y. Chang et al., "A data-driven crop model for maize yield prediction," *Communications Biology*, vol. 6, p. 439, 2023, doi: 10.1038/s42003-023-04833-y. [Online]. Available: <https://pmc.ncbi.nlm.nih.gov/articles/PMC10121691/>. [Accessed: Jan. 9, 2025].
- [27] J. Ma et al., "Skillful seasonal predictions of continental East-Asian summer rainfall by integrating its spatio-temporal evolution," *Nature Communications*, vol. 16, no. 1, p. 273, 2025, doi: 10.1038/s41467-024-55271-1. [Online]. Available: <https://www.nature.com/articles/s41467-024-55271-1>. [Accessed: Jan. 9, 2025].
- [28] Dataset: Uganda: Rainfall Indicators at Subnational Level. [Online]. Available: <https://data.humdata.org/dataset/uga-rainfall-subnational>. [Accessed: Jan. 9, 2025].
- [29] Exploratory Data Analysis Code. [Online]. Available: <https://www.kaggle.com/code/ronnieatuhaire/proposal>. [Accessed: Jan. 9, 2025].
- [30] FAO 2024 - Uganda Investment Proposal. [Online]. Available: <https://www.fao.org/hand-in-hand/hih-IF-2024/uganda/en>. [Accessed: Jan. 9, 2025].



RONALD ATUHAIRE is a Computer Science student at Makerere University, driven by a passion for using technology to solve societal challenges. He co-founded MpaMpe, a blockchain-powered crowdfunding platform that promotes transparency, inclusivity, and accountability. Under his leadership, MpaMpe raised over 5,000 USD, earning multiple accolades including the Student Innovation Challenge at Makerere University and the Women in Fintech Hackathon.

Ronald has been recognized globally, with honors such as the Global Undergraduate Awards (GUA) 2024, MTN MoMo Hackathon, and being a Top 50 Global Finalist in the Google Students Solution Challenge. He is also the winner of the Canva AI Integrations Hackathon and Africa Business Marketplace Simulation.

As Lead Researcher at Farm Zenith, he has advanced agricultural resilience to climate change and poverty, publishing the paper "Transparent Multimodelling for Climatic Geo Intelligence in Predicting Food Security," which was recognized in GUA. Ronald has contributed globally as a Microsoft and Wolfram Ambassador, Twilio Champion, Notion Campus Lead, and Google Developer Student Clubs Lead (now GDG On Campus).

Honored with fellowships such as the Millennium Fellowship, Clinton Global Initiative Fellowship, and Tech Savvy Fellowship, Ronald is committed to using his expertise to empower communities and foster social transformation. He actively engages in global tech communities, including DevFest, PyCon Uganda, and blockchain events, to share knowledge and inspire peers.



EDWARD KABOGGOZA is a computer science researcher specializing in AI-driven solutions for agricultural resilience with a keen interest in software development and artificial intelligence. He has a strong foundation in Python and real-time communication technologies and is focused on building scalable and efficient systems. His areas of interest include AI-driven solutions, cloud computing, and system optimization, with a particular emphasis on leveraging machine learning for accessibility and communication.

Edward enjoys working on projects that integrate speech-to-text, translation, and text-to-speech technologies to enhance global communication and education. He is deeply committed to research and continuous learning, always seeking innovative ways to solve real-world challenges through technology.

In his academic and personal pursuits, Edward continues to contribute to the development of advanced systems that aim to improve accessibility and facilitate better communication globally.



SSEMAGANDA GEORGE is a Computer Science student and researcher at Makerere University, with a strong passion for tech-driven sustainable innovation. He holds a Diploma in Electrical Engineering and has certifications in cybersecurity, data protection, energy access, and innovation, giving him a multidisciplinary approach to problem-solving.

George participated in the UN Datathon 2023 and was a Guild presidential aspirant at Makerere University in 2024. As Innovations Lead for Google Developer Groups (GDG) on Campus, he works on Google tech projects to address real-world challenges. He has published research on food security prediction using AI, aimed at optimizing crop yields for farmers, and co-founded DirtTrails Safaris, a responsible tourism initiative. Additionally, George volunteered at MpaMpe Digital Services, where he contributed to crowdfunding efforts to support underserved communities.

With expertise in technology, leadership, and entrepreneurship, George is committed to bridging the gap between technology and human needs, contributing to Africa's digital transformation.

...